Journal of Solid State Chemistry 184 (2011) 2061–2065

Contents lists available at ScienceDirect

Journal of Solid State Chemistry

journal homepage: www.elsevier.com/locate/jssc

Preparation, crystal structure, and superconductive characteristics of new oxynitrides $(Nb_{1-x}M_x)(N_{1-y}O_y)$ where M=Mg, Si, and $x \approx y$

Yoshio Ohashi [a], Teruki Motohashi [a], Yuji Masubuchi [a], Toshihiro Moriga [b], Keiichiro Murai [b], Shinichi Kikkawa [a,*]

[a] Graduate School of Engineering, Hokkaido University, N13W8, Kita-ku, Sapporo 060-8628, Japan
[b] Graduate School of Advanced Technology and Science, The University of Tokushima, 2-1 Minamijyousanjima-cho, Tokushima 770-8506, Japan

ARTICLE INFO

Article history:
Received 18 April 2011
Received in revised form
1 June 2011
Accepted 2 June 2011
Available online 12 June 2011

Keywords:
New compound
Oxynitride
Crystal structure
Neutron diffraction
EXAFS
Superconductor

ABSTRACT

New niobium oxynitrides containing either magnesium or silicon were prepared at 1000 °C by ammonia nitridation of oxide precursors obtained via the citrate route. The products had rock-salt type crystal structures. Crystallinity was improved by annealing in 0.5 MPa N_2 and the final compositions were $(Nb_{0.95}Mg_{0.05})(N_{0.92}O_{0.08})$ at 1500 °C and $(Nb_{0.87}Si_{0.09}\square_{0.04})(N_{0.87}O_{0.13})$ at 1200 °C. The magnesium and oxide ions partially co-substitute the niobium and nitride ions in the octahedral sites of the δ-NbN lattice, respectively. Silicon ions were also successfully doped together with oxide ions into the rock-salt type NbN lattice. The Si doped product exhibited relatively large displacement at the octahedral sites and was accompanied by a small amount of cation vacancies. Superconductivity was improved by annealing to obtain critical temperatures/volume fractions of T_c=17.6 K/100% for Mg- and T_c=16.2 K/95% for the Si-doped niobium oxynitrides.

1. Introduction

The use of oxynitrides as functional materials in applications such as white LED phosphors [1,2], photocatalysis [3,4], inorganic pigments [5,6], and dielectric materials [7] is becoming increasingly important. The optical response of these materials in the UV–visible range is induced by the introduction of more covalent nitride ions into the oxide crystal lattice [8]. Asymmetric coordination of these anions around the cations in the structure is required to obtain large dielectric properties [9]. The distribution of both oxide and nitride anions affects the dielectric properties of the resultant oxynitrides. Oxynitrides of niobium or tantalum have been reported to exhibit different crystal structures according to the cations present in the structure. There are several types of oxynitrides with AMO_2N or $RMON_2$ perovskite type crystal structures, where A, R, and M are alkaline earth, rare earth, and tantalum or niobium ions, respectively [10–12]. Large dielectric constants have been observed for $SrTaO_2N$ and $BaTaO_2N$, [7] and colossal magnetoresistance was reported for $EuNbO_{2+x}N_{1-x}$ [13]. Pyrochlore-type structure nitrided products, $R_2Ta_2O_5N_2$, where R=Nd to Gd, and defect fluorite-type $RTa(O,N,\square)_4$ for smaller R=Tb to Lu have also been reported [12]. Both defect rock-salt and Nb_5N_6-type crystal structures have been reported for Li–Nb [14] and Mn–Nb oxynitrides [15], similar to the pristine niobium nitrides.

Niobium aluminum oxynitride was recently prepared by ammonolysis of an oxide precursor obtained through the citrate route [16]. The refined chemical composition was $(Nb_{0.60}Al_{0.08}\square_{0.32})(N_{0.79}O_{0.21})$ with vacancies ordered in the rock-salt type crystal structure. The compound was transformed to $(Nb_{0.89}Al_{0.11})(N_{0.84}O_{0.16})$ with a simple rock-salt structure after annealing in nitrogen at 1500 °C [17], and exhibited superconductivity with a critical temperature T_c, of 17.3 K, where Al^{3+} and O^{2-} ions were assumed to be doped together into the rock-salt type δ-NbN structure.

Several types of niobium nitrides have been reported [18–24]. α-NbN_x ($0 \le x \le 0.40$) is a superconductor with T_c=4.0–9.2 K. β-Nb_2N crystallizes in a hexagonal ε-Fe_2N type structure with T_c=3.8–8.6 K. Higher nitrides, such as γ-Nb_4N_3 (T_c=12–15 K), δ-NbN (T_c=14.7–17.7 K), and Nb_4N_5 (T_c=8.5–10 K) also crystallize with a rock-salt type structure. δ′-NbN of NiAs type, and ε-NbN of TiP type are non-superconductors. Many superconductive solid solution derivatives have been prepared by partial substitution of Nb in δ-NbN with transition metals by either ammonolysis, high temperature reaction under nitrogen, or solid state reaction of the transition metal nitrides [25,26]. The T_c values of these derivatives are intermediate compared with their end members due to the hybridization of the d-orbitals. Slight enhancement of T_c was observed for the solid solution formed between δ-NbN and TiC

* Corresponding author. Fax: +81 11 706 6739.
E-mail address: kikkawa@eng.hokudai.ac.jp (S. Kikkawa).

0022-4596/$ - see front matter © 2011 Elsevier Inc. All rights reserved.
doi:10.1016/j.jssc.2011.06.003

with $T_c \approx 18.0$ K [26]. Apart from $(Nb_{0.89}Al_{0.11})(N_{0.84}O_{0.16})$, there have been no reports on superconductive δ-NbN doped with main group elements, especially codoped with oxide ions.

In the present investigation, magnesium or silicon analogs were prepared by substituting aluminum in the Nb–Al oxynitride. Mg, Al, and Si are neighboring elements in the periodic table, although their valencies, atomic radii, and coordination numbers are different and affect the crystal and electronic structures differently. The crystal structures and superconductivity of niobium oxynitrides doped with either Mg or Si were compared with those of $(Nb_{0.89}Al_{0.11})(N_{0.84}O_{0.16})$ [17].

2. Experimental

Amorphous oxide precursors were obtained by the following method. $NbCl_5$ (Sigma-Aldrich, 99.9%) was dissolved with either $MgCl_2 \cdot 6H_2O$ (Kanto Chemicals, 99.0%) or $Si(OC_2H_5)_4$ (Aldrich, 98.0%) in a molar ratio of $(1-x)$:x, where x=0, 0.05, 0.1,…,1.0, in 20 mL of anhydrous ethanol in which an equimolar amount of citric acid (Wako Pure Chemicals) was added as a complexing agent. The viscous material was fired at 350 °C for 1 h in air and the resultant oxide powders were ground. The oxide precursors were nitrided in an alumina boat with an ammonia (Sumitomo Seika Chemicals, 99.9%) flow of 50 mL/min at 1000 °C for 10 h. After the ammonolysis reaction, the samples were cooled to room temperature and the residual ammonia in the silica glass reaction tube was purged by nitrogen gas flow. The as-nitrided products were thermally annealed at 1200 or 1500 °C for 3 h in 0.5 MPa N_2 using a graphite furnace (High Multi 500, Fuji Dempa Kogyo).

The as-nitrided and post-annealed products were characterized using X-ray diffraction (XRD), neutron diffraction (ND), chemical analysis, and magnetic susceptibility measurements. XRD patterns were collected using a diffractometer (Ultima IV, Rigaku) with monochromatized Cu$K\alpha$ radiation over the 2θ angular range of 5.0–120.0° with a step size of 0.02°. ND measurements were carried out using the high resolution powder diffractometer (HRPD; HERMES, Institute for Materials Research, Tohoku University) installed at the JRR-3M reactor of the Japan Atomic Energy Agency (JAEA) [27]. A neutron beam with a wavelength of 0.184843 nm was obtained with the 331 reflection of a Ge monochromator. ND was measured over the 2θ angular range of 3.0–152.9° with a step size of 0.1° using approximately 3 g of the oxynitride product filled in a vanadium cylinder. The crystal structure of the products was refined by the Rietveld method using RIETAN2000 software [28]. The anionic composition was determined using an oxygen/nitrogen combustion analyzer (EMGA-620W, Horiba) that was calibrated using Gd_2O_3 (Wako Pure Chemicals, 99.99%, fired at 1000 °C for 10 h prior to use) and Si_3N_4 (The Ceramic Society of Japan, JCRM R 003) as standard materials. Magnetic susceptibility was measured using a superconducting quantum interference device (SQUID) magnetometer (MPMS-5S, Quantum Design) in the temperature range of 2–50 K under a magnetic field of 5 mT. Nb K-edge X-ray absorption was measured in transmission mode at the NW-10A beamline at the Photon Factory, High Energy Accelerator Research Organization (KEK), Tsukuba. The spectrum was analyzed using REX2000 software (Rigaku) with n=3 in the k-range of 0.30–1.10 nm [29].

3. Results and discussion

3.1. Niobium–magnesium oxynitrides

The product of ammonolysis at 1000 °C without the Mg additive was rock-salt type Nb(N,O) contaminated with a small amount of hexagonal δ′- or ε-NbN, as shown in Fig. 1 [30]. Similar rock-salt type products were obtained for those precursors containing various amounts of Mg. The amount of the hexagonal NbN impurity was decreased with the Mg content (x) and another impurity of MgO appeared at x=0.10. The lattice parameter was a=0.4437 nm at x=0, which is comparable to the literature value of a=0.442 nm for Nb(N,O) [30]. The lattice parameter continuously decreased with x to a=0.4403 nm at x=0.20. $Nb_{1-x}Mg_x$ oxynitrides were assumed to be present in the narrow range of $x < 0.20$.

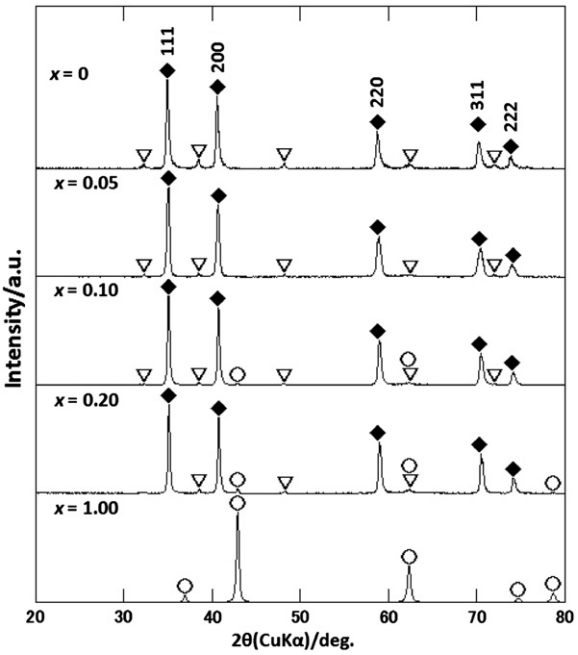

Fig. 1. X-ray diffraction patterns for the ammonolysis products of $Nb_{1-x}Mg_x$ compositions nitrided at 1000 °C. Filled diamonds, open triangles, and circles represent diffraction peaks related to rock-salt type, hexagonal δ′- or ε-NbN, and MgO, respectively.

Crystallinity was improved by post-annealing of the ammonolysis products at 1500 °C in nitrogen atmosphere, as shown by the XRD patterns in Fig. 2. The NbN impurity disappeared; however, MgO was observed above x=0.10. The lattice parameter at x=0.10 was reduced to a=0.4414 nm. The solid solution limit was very narrow and was estimated to be between x=0.05 and 0.10.

The crystal structure of the post-annealed $Nb_{0.95}Mg_{0.05}$ oxynitride was refined using the powder XRD data in the space group Fm-3m with a=0.4419(1) nm. The composition assumed in the refinement was $(Nb_{0.95}Mg_{0.05})(N_{0.92}O_{0.08})$, as determined by the chemical analysis on the amount of nitrogen and oxygen. Nb/Mg and N/O were statistically distributed in 4a and 4b sites, respectively. The refined displacement factors of 4a site were in agreement with the literature values [15,17], as shown in Table 1, under the constraints of B(Nb)=B(Mg) and B(O)=B(N). Both cations and anions were octahedrally coordinated to each other with a bond length of 0.2209 nm, which is comparable to the bond lengths of 0.2196–0.2216 nm reported between niobium and anions in δ-Nb(N,O) [16,24]. This length is slightly longer than the 0.2107 nm for the Mg–O bond length in MgO [31] and 0.2084–0.2179 nm for the Mg–N bond length in Mg_3N_2 [32].

3.2. Niobium–silicon oxynitrides

After ammonolysis at 1000 °C, the nitride product without silicon additive was rock-salt type Nb(N,O) containing hexagonal δ′- or ε-NbN impurities, as shown in Fig. 3, similar to the case for magnesium addition. The crystallinity decreased in the main

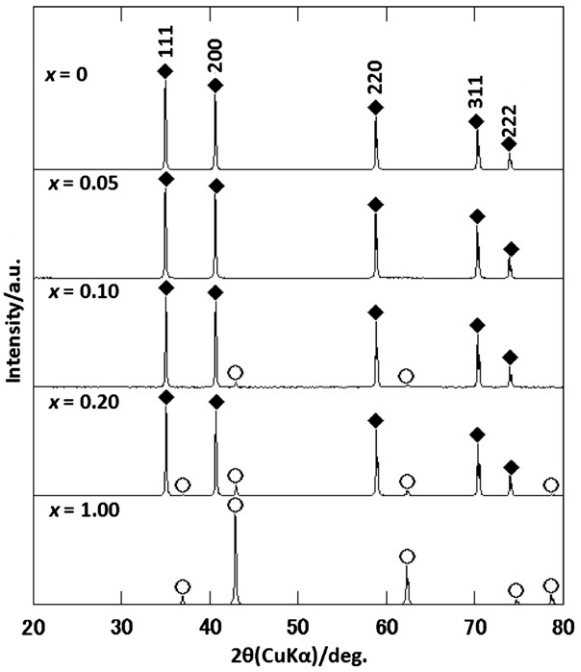

Fig. 2. XRD patterns for $Nb_{1-x}Mg_x$ oxynitrides post-annealed at 1500 °C in nitrogen. Filled diamonds and open circles represent diffraction peaks related to the rock-salt type products and MgO.

Table 1
Structural parameters of $(Nb_{0.95}Mg_{0.05})(N_{0.92}O_{0.08})$ post-annealed at 1500 °C refined by the Rietveld method using powder XRD data.

Atom	Site	g	x	y	z	$B/\times 10^{-2}$ nm^2
Nb	4*a*	0.95	0	0	0	0.07(2)
Mg	4*a*	0.05	0	0	0	0.07(2)
O	4*b*	0.08	1/2	1/2	1/2	0.89
N	4*b*	0.92	1/2	1/2	1/2	0.89

Space group: *Fm*-3*m*, $a=0.4419(1)$ nm, $V=8.629(2)\times 10^{-29}$ m^3, $WR_p=10.78\%$, Re=8.10%, S=1.17.

phase with increase in silicon content x', and the impurity disappeared at $x'=0.10$. The lattice parameter was reduced to around $a=0.437$ nm in the compositional range of $0.05\le x'\le 0.10$. There was no crystalline impurity detected in the product with $x'=0.10$. The nitrided product without niobium at $x'=1.00$ was X-ray amorphous.

The ammonolysis products were annealed in nitrogen at 1200 °C after grinding. Fig. 4 shows that crystallinity of the silicon containing products was improved after annealing. The lattice parameter was expanded to approximately $a=0.441$ nm above $x'=0.10$ by post-annealing and the values were independent of the silicon content x' up to $x'=0.70$. Amorphous SiO_2 may be present as an impurity and its content would be increased with x' assuming a solid solution limit at around $x'=0.10$. Slight crystallization of δ-NbN and cristobalite was observed after post-annealing at 1500 °C.

Both the cation and the anion distributions were refined in the rock-salt type structure using Rietveld refinement of neutron diffraction data of the product prepared from a starting composition of $Nb_{0.90}Si_{0.10}$ that was post-annealed at 1200 °C. The original refined result was $(Nb_{0.86(3)}Si_{0.14(3)})(N_{0.89(2)}O_{0.11(2)})$; however, the silicon content was unreasonable because it was greater than x' in the starting composition. Another refinement was performed assuming that the cation sites were occupied by niobium and silicon in a 9:1 starting composition ratio together with some amount of vacancies.

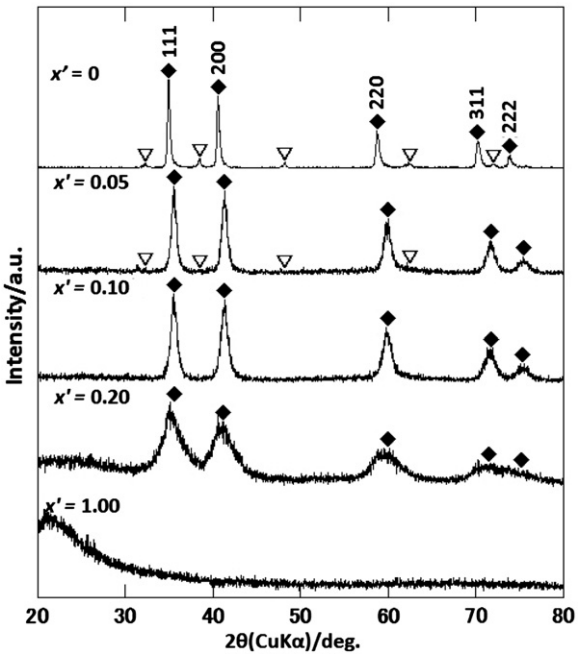

Fig. 3. XRD patterns for the ammonolysis products of $Nb_{1-x'}Si_{x'}$ compositions nitrided at 1000 °C. Filled diamonds and open triangles represent diffraction peaks related to the rock-salt type and hexagonal δ′- or ε-NbN.

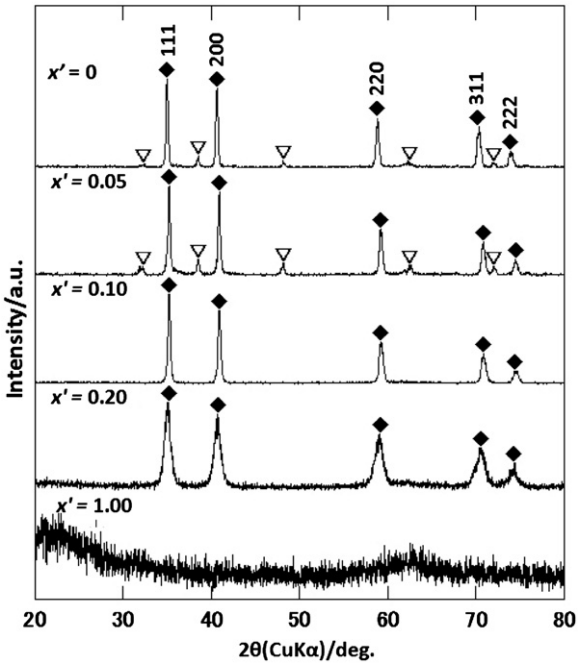

Fig. 4. XRD patterns for $Nb_{1-x'}Si_{x'}$ oxynitrides post-annealed at 1200 °C in nitrogen. Filled diamonds and open triangles represent diffraction peaks related to the rock-salt type products and hexagonal δ′- or ε-NbN.

The converged result was $(Nb_{0.87(2)}Si_{0.09(0)}\square_{0.04(2)})(N_{0.87(2)}O_{0.13(2)})$, as shown in Table 2. The distance between the cations and anions was 0.2205 nm and comparable to those reported (0.2196–0.2216 nm) for other niobium oxynitrides [16,24]. The Si–O bond distance is much longer than that of 0.160–0.161 nm in quartz [33] and Si–N of 0.172–0.175 nm in α-Si_3N_4 [34]. It is even longer than the Si–O distance of 0.176–0.181 nm in stishovite, in which Si ions are octahedrally coordinated with oxide ions in a rutile structure [35]. The displacement factor for the 4*a* site was 0.53×10^{-2} nm^2, which is much larger than that in $(Nb_{0.95}Mg_{0.05})(N_{0.92}O_{0.08})$, although the value for

Table 2
Structural parameters of $(Nb_{0.87}Si_{0.09}\square_{0.04})(N_{0.87}O_{0.13})$ post-annealed at 1200 °C refined under the constraints of g(Si)=0.1 g(Nb) and g(O)+g(N)=1 by the Rietveld method using neutron diffraction data.

Atom	Site	g	*x*	*y*	*z*	B/$\times 10^{-2}$ nm^2
Nb	4*a*	0.87(2)	0	0	0	0.53(5)
Si	4*a*	0.09	0	0	0	0.53(5)
O	4*b*	0.13(2)	1/2	1/2	1/2	1.3(4)
N	4*b*	0.87(2)	1/2	1/2	1/2	1.3(4)

Space group: *Fm*-3*m*, $a=0.4409(1)$ nm, $V=8.571(2)\times 10^{-29}$ m^3, $WR_p=6.40\%$, Re=3.25%, S=1.97.

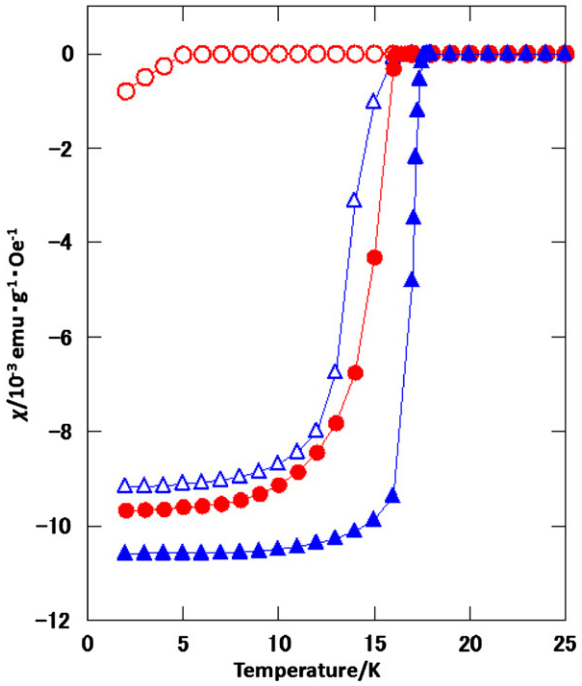

Fig. 5. Magnetic susceptibility of the $Nb_{0.95}Mg_{0.05}$ (triangles) and $Nb_{0.95}Si_{0.10}$ (circles) oxynitrides as a function of temperature measured with zero field cooling. Open and filled marks correspond to the ammonolysis and post-annealed products, respectively.

the anionic 4*b* site was reasonable. It might be caused mainly by the defects in the (Nb/Si) site. The doped silicon ions might be slightly shifted from the regular octahedral 4*a* site in the rock-salt type crystal lattice.

3.3. Superconductive characteristics of the doped niobium oxynitrides

The magnetic susceptibility of the as-nitrided and post-annealed products of $(Nb_{0.95}Mg_{0.05})$ and $(Nb_{0.90}Si_{0.10})$ oxynitrides was measured. The as-nitrided Mg-doped oxynitride product exhibited superconductivity at $T_c=15$ K and a volume fraction of 89%, as depicted in Fig. 5. The post-annealed product showed an improvement in the superconductivity to $T_c=17.6$ K and 100% volume fraction. The superconducting characteristics were different in the Si-doped products from the $(Nb_{0.95}Mg_{0.05})$ oxynitrides. The as-nitrided $(Nb_{0.90}Si_{0.10})$ oxynitride had $T_c=5$ K and 8% volume fraction, probably due to insufficient crystallization in the compound. The superconductivity was significantly elevated to $T_c=16.2$ K and 95% volume fraction after post-annealing, although these values were still less than those observed in the post-annealed niobium oxynitrides doped with either Mg or Al.

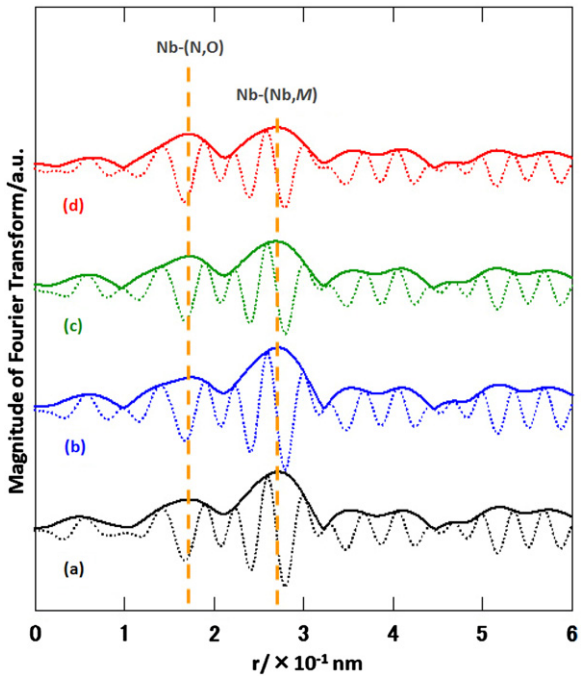

Fig. 6. Fourier transforms of the Nb K-edge EXAFS for (a) Nb(N,O), (b) $(Nb_{0.95}Mg_{0.05})(N_{0.92}O_{0.08})$, (c) $(Nb_{0.89}Al_{0.11})(N_{0.84}O_{0.16})$, and (d) $(Nb_{0.87}Si_{0.09}\square_{0.04})(N_{0.87}O_{0.13})$.

X-ray absorption spectroscopy was applied to study the Nb K-edge absorption and the Fourier transform of the extended X-ray absorption fine structure (EXAFS) for the post-annealed products. The K-edge shape was practically the same among the doped and undoped niobium oxynitrides, and was also very similar to that reported for NbN [36]. The first and the second nearest neighbors around Nb were observed at around 0.17 and 0.27 nm, respectively, for both the doped and undoped niobium oxynitrides, as presented in Fig. 6. The atomic distances reported in the literature are 0.22 nm for Nb–(O,N) and 0.35 nm for Nb–Nb [16,24,30]. The peak profile was slightly broader for the first and the second nearest neighbors in $(Nb_{0.87}Si_{0.09}\square_{0.04})(N_{0.87}O_{0.13})$ than those for the other doped and undoped niobium oxynitrides, probably because doping with silicon resulted in a relatively large displacement at the octahedral 4*a* site in the crystal structure refinement. The imperfect crystal structure might reduce the superconductive characteristics rather than a change in the electronic structure by codoping of oxide ions with Mg, Al, or Si into the NbN crystal lattice. The oxygen contents were comparable to the amount of total cationic dopants in the δ-NbN lattice in the respective doped oxynitrides: $(Nb_{0.95}Mg_{0.05})(N_{0.92}O_{0.08})$, $(Nb_{0.89}Al_{0.11})(N_{0.84}O_{0.16})$, and $(Nb_{0.87}Si_{0.09}\square_{0.04})(N_{0.87}O_{0.13})$. The amounts of extra formal charge from M–O doping to the NbN lattice were −0.06, +0.01, and +0.10 for M=Mg, Al, and Si in the above compositions, respectively. The residual charges in the doped oxynitrides were calculated as +0.03, +0.16, and +0.10 for M=Mg, Al, and Si, respectively, assuming that the formal valencies of niobium and nitrogen were +3 and −3, even in the nonstoichiometric NbN host lattice. The change of the observed T_c-values in the Mg-, Al-, and Si-doped niobium oxynitrides, $T_c=17.6$, 17.3, and 16.2 K, does not correspond to the estimation using the rigid band model: $k_BT_c=1.14\omega_D\exp[-1/N(0)V]$, where k_B, ω_D, $N(0)$, and V are the Boltzmann constant, the Debye frequency, the density of states at the Fermi level, and the interaction parameter, respectively [36]. The change in the residual charge, which may be related to $N(0)$, did not correspond

to the variation of T_c among the Mg-, Al-, and Si-doped niobium oxynitrides.

The superconducting coherence length can be assumed as the minimum width of the intermediate layer between non-superconducting and superconducting materials [37,38]. Superconductivity requires a grain size larger than the coherence length. The crystallite sizes, estimated from the XRD line broadening of the 220 diffraction, were 43, 27, and 16 nm for the Mg-, Al-, and Si-doped niobium oxynitrides, respectively. The coherence length has been assumed to be 5.0 nm in NbN [39]. Therefore, a smaller crystallite size in an imperfect crystal structure may reduce the T_c value together with the volume fraction in a doped niobium oxynitride.

4. Conclusion

Mg- and Si-doped niobium oxynitrides were synthesized by post-annealing of the ammonolysis products in nitrogen. The oxynitrides crystallized with a rock-salt type crystal structure similar to δ-NbN and exhibited superconductivity of $T_c > 16$ K. Approximately 10 at% of the nitride ions was substituted with oxide ions, together with substitution of niobium for only Mg^{2+} or Si^{4+} with cationic vacancies. Relatively large displacement of the cation site was observed for the Si-doped niobium oxynitride. The superconducting T_c-values were comparable to 17.6 K in Nb(N,O) and were slightly reduced in the Si-doped niobium oxynitride with structural imperfections.

Acknowledgments

This research was partly supported by a Grant-in-Aid for Scientific Research (Kakenhi (A) #21245047) from the Japan Society for the Promotion of Science (JSPS). Neutron diffraction and X-ray absorption experiments were performed under approval of 9876K for the JRR-3M reactor from JAEA, and under approval of Proposal No. 2010G135 from the Photon Factory Advisory Committee, respectively. T.M. acknowledges financial support from the Global COE Program (Project No. B01: "Catalysis as the Basis for Innovation in Materials Science") from the Ministry of Education, Culture, Sports, Science and Technology (MEXT), Japan.

References

[1] R.–J. Xie, M. Mitomo, K. Uheda, F.F. Xu, Y. Akimune, J. Am. Ceram. Soc. 85 (2002) 1229–1234.
[2] J.W.H. van Krevel, J.W.T. van Rutten, H. Mandal, H.T. Hintzen, R. Metselaar, J. Solid State Chem. 165 (2002) 19–24.
[3] K. Maeda, K. Domen, J. Phys. Chem. C111 (2007) 7851–7861.
[4] K. Maeda, H. Hashiguchi, H. Masuda, R. Abe, K. Domen, J. Phys. Chem. C112 (2008) 3447–3452.
[5] M. Jansen, H.P. Letschert, Nature 404 (2000) 980–982.
[6] F. Tessier, R. Marchand, J. Solid State Chem. 171 (2003) 143–151.
[7] Y.-I. Kim, P.M. Woodward, K.Z.B. Kishi, C.W. Tai, Chem. Mater. 16 (2004) 1267–1276.
[8] F. Tessier, P. Maillard, F. Cheviré, K. Domen, S. Kikkawa, J. Ceram. Soc. Jpn 117 (2009) 1–5.
[9] M. Yang, J. Oró-Solé, J.A. Rodgers, A.B. Jorge, A. Fuertes, J.P. Attfield, Nat. Chem. 3 (2011) 47–52.
[10] R. Marchand, in: K.A. Gshneider Jr., L. Eyling (Eds.), Hand Book on the Physics and Chemistry of Rare Earths, vol. 25, Elsevier, 1998, pp. 51–99.
[11] P. Maillard, F. Tessier, E. Orhan, F. Cheviré, R. Marchand, Chem. Mater. 17 (2005) 152–156.
[12] S. Kikkawa, T. Takeda, A. Yoshiasa, P. Maillard, F. Tessier, Mater. Res. Bull. 43 (2008) 811–818.
[13] A. Belen Jorge, J. Oró-Solé, A.M. Bea, N. Mufti, T.T.M. Palstra, J.A. Rodgers, J.P. Attifield, A. Fuertes, J. Am. Chem. Soc. 130 (2008) 12572–12573.
[14] F. Tessier, R. Assabaa, R. Marchand, J. Alloys Compd 262–263 (1997) 512–515.
[15] A. Tyutyunnik, J. Grins, G. Svensson, J. Alloys Compd 278 (1998) 83–91.
[16] S. Yamamoto, Y. Ohashi, Y. Masubuchi, T. Takeda, T. Motohashi, S. Kikkawa, J. Alloys Compd 482 (2009) 160–163.
[17] Y. Ohashi, T. Motohashi, Y. Masubuchi, S. Kikkawa, J. Solid State Chem. 183 (2010) 1710–1714.
[18] R.W. Guard, J.W. Savage, D.G. Swartout, Trans. Metall. Soc. AIME 239 (1967) 643–649.
[19] E.F. Skelton, M.R. Skokan, E. Cukauskas, J. Appl. Cryst. 14 (1981) 51–57.
[20] P. Fabbricatore, P. Fernandes, G.C. Gualco, F. Merlo, R. Musenich, R. Parodi, J. Appl. Phys. 66 (1989) 5944–5949.
[21] B. Scheerer, J. Cryst. Growth 49 (1980) 61–66.
[22] R. Berger, W. Lengauer, P. Ettmayer, J. Alloys Compd 259 (1997) 9–13.
[23] A.V. Linde, R.-M. Marin-Ayral, D. Granier, F. Bosc-Rounessac, V.V. Grachev, Mater. Res. Bull. 44 (2009) 1025–1030.
[24] N. Terao, J. Less-Common Met. 23 (1971) 159–169.
[25] K. Hechler, G. Horn., G. Otto, E. Saur, J. Low Temp. Phys. 1 (1969) 29–43.
[26] N. Pessall, R.E. Gold, H.A. Johansen, J. Phys. Chem. Solids 29 (1968) 19–38.
[27] K. Ohoyama, T. Kanouchi, K. Nemoto, M. Ohashi, T. Kajitani, Y. Yamaguchi, Jpn. J. Appl. Phys. 37 (1998) 3319–3326.
[28] F. Izumi, T. Ikeda, Mater. Sci. Forum 321–324 (2000) 198–203.
[29] T. Taguchi, T. Ozawa, H. Yashiro, Phys. Scr. T115 (2005) 205–206.
[30] JCPDS 12-256.
[31] V.G. Tsirelson, A.S. Avilov, Y.A. Abramov, E.L. Belokoneva, R. Kitaneh, D. Feil, Acta Cryst. B54 (1998) 8–17.
[32] D.E. Partin, D.J. Williams, M. O'Keeffe, Solid State Chem 132 (1997) 56–59.
[33] P. Norby, J. Appl. Cryst. 30 (1997) 21–30.
[34] H. Toraya, J. Appl. Cryst. 33 (2000) 95–102.
[35] R.J. Hill, M.D. Newton, G.V. Gibbs, J. Solid State Chem. 47 (1983) 185–200.
[36] Y. Wakai, T. Hara, K.K. Bando, N. Ichikuni, S. Shimazu, Top. Catal 52 (2009) 1517–1524.
[37] E.M. Savitskii, V.V. Baron, Yu.V. Efimov, M.I. Bychkova, L.F. Myzenkova, Superconducting Materials, Plenum Press, New York, 1973, p. 17.
[38] C.P. Poole, T. Datta, H.A. Farach, Copper oxide Superconductors, John Wiley & Sons, Toronto, 1988, p. 30.
[39] S. Perkowitz, Phys. Rev. B 25 (1982) 3420–3423.